Insect Biochemistry and Molecular Biology 107 (2019) 39–45

Contents lists available at ScienceDirect

Insect Biochemistry and Molecular Biology

journal homepage: www.elsevier.com/locate/ibmb

The *N*-glycome of the hemipteran pest insect *Nilaparvata lugens* reveals unexpected sex differences

Freja Scheys[a,b,2], Kristof De Schutter[a,2], Ying Shen[a,b], Na Yu[a,b,1], Nicolas Smargiasso[c], Edwin De Pauw[c], Els J.M. Van Damme[b], Guy Smagghe[a,*]

[a] Department of Plants and Crops, Faculty of Bioscience Engineering, Ghent University, Coupure Links 653, 9000, Ghent, Belgium
[b] Department of Biotechnology, Faculty of Bioscience Engineering, Ghent University, Coupure Links 653, 9000, Ghent, Belgium
[c] Mass Spectrometry Laboratory, Molecular Systems Research Unit, University of Liège, Allée du 6 Août 11, 4000, Liège, Belgium

ARTICLE INFO

Keywords:
N-Glycosylation
Pest insect
Nilaparvata lugens
Mass spectrometry
qPCR

ABSTRACT

The brown planthopper, *Nilaparvata lugens*, is a model species for hemimetabolous development and the most important pest insect in rice, which is the major staple crop for about half of the world population. Despite its importance, little is known of the *N*-glycosylation process in this insect. Here we report on the *N*-glycome for the post-embryonic stages of *N. lugens*, revealing unique features that are different from the holometabolous insect models, as the fruit fly *Drosophila melanogaster* and the beetle *Tribolium castaneum*. Analysis of the *N*-glycan fingerprint for male and female adults showed sex-specific *N*-glycosylation in insects. Specifically, the female adults progress towards a unique glycan profile with a striking increase in high mannose *N*-glycans. The *N*-glycome of *N. lugens* contributes to study pathways differentiating between sexes, and the results shed light on the evolution and differences in development between primitive hemimetabolous insects and more advanced holometabolous insects. The data are discussed in relation to potential function(s) in development and sex specificity.

1. Introduction

Along with DNA, RNA and proteins, carbohydrates represent the fundamental biomolecules of a cell. Glycosylation refers to the enzymatic process that attaches carbohydrates or glycans to proteins or other organic molecules, and represents an important co-translational and/or post-translational modification, since glycans serve a range of structural and functional roles (Dwek, 1996; Ohtsubo and Marth, 2006; Endo, 2009; Walski et al., 2017). The variety in monosaccharides and glycosyltransferases available to build *N*-glycans will result in a wide range of carbohydrate chains, differing in size and structure, and modulating biological diversity and complexity (Varki and Kornfield, 2017).

The first steps of the *N*-glycosylation pathway are highly conserved in eukaryotic cells and involve the assembly of the dolichol-linked *N*-glycan precursor at the membrane of the endoplasmic reticulum (ER), followed by the transfer of the $GlcNAc_2Man_9Glc_3$ oligosaccharide to the nascent polypeptide (Altmann, 1996). After deglucosylation, the *N*-glycan will be subjected to initial trimming by class I α-mannosidases (Man1a/b) during the transport of the glycoprotein to the Golgi apparatus. During the further processing of the carbohydrate chain in the Golgi, differences between kingdoms occur (De Pourcq et al., 2010). In fungi, the *N*-glycans are elongated leading to complicated hypermannosylated glycoforms, whereas in the animal kingdom glycan structures differ between taxa. In mammalian cells, the *N*-glycans are processed to complex type glycan structures (De Pourcq et al., 2010), while in insect cells, oligomannose and (core fucosylated) paucimannosidic *N*-glycans are the most common structures (Fabini et al., 2001; Aoki et al., 2007; Ten Hagen et al., 2009; Kurz et al., 2015). Though these glycans can be elongated by the addition of galactose (Gal), *N*-acetylgalactosamine (GalNAc) and/or sialic acid (Sia) residues, these complex glycans are typically low abundant in invertebrates (Wilson, 2002; Schiller et al., 2012).

Although insects are the largest animal taxon on earth, with an enormous genetic and phenotypic diversity (Sanderson, 2008), glycan studies have only focused on holometabolous insects such as the fruit

* Corresponding author.
E-mail address: Guy.Smagghe@UGent.be (G. Smagghe).
[1] Current address: Key Laboratory of Integrated Management of Crop Diseases and Pests (Ministry of Education), College of Plant Protection, Nanjing Agricultural University, Weigang 1, Nanjing 210095, China.
[2] Equal first authors.

https://doi.org/10.1016/j.ibmb.2019.01.008
Received 25 October 2018; Received in revised form 13 January 2019; Accepted 24 January 2019
Available online 28 January 2019
0965-1748/

fly *Drosophila melanogaster* (Fabini et al., 2001; Aoki et al., 2007; Ten Hagen et al., 2009; North et al., 2006) and other dipteran insects (Kurz et al., 2015), beetles (Dönitz et al., 2014; Walski et al., 2016), moths (Stanton et al., 2017), caterpillars (Kajihura et al., 2015; Mabashi-Asazuma et al., 2015; Soya et al., 2016) and bees (Kubelka et al., 1993, 1995). At present, no information is available on the *N*-glycosylation process in hemipteran insects.

The hemipteran insect *Nilaparvata lugens* or the brown planthopper (BPH) is commonly investigated as a model for hemimetabolous insects. In addition, *N. lugens* is one of the most notorious pest insects in rice, where outbreaks of BPH in rice fields lead to enormous economic losses each year (Kshirod and Suk-Man, 2010; Bao et al., 2013). Being a sap-sucking pest insect, *N. lugens* causes direct damage to the rice plant by feeding on the rice phloem, inducing a condition called 'hopperburn'. Furthermore, BPH acts as a vector for rice viruses like the rice grassy stunt virus and the ragged stunt virus, causing indirect plant damage (Li et al., 2011).

This study focusses on the *N*-glycome of *N. lugens*, a model insect for hemimetabolous post-embryonic development. Analysis of the *N*-glycan profile of the nymphal stages revealed important discrepancies with holometabolous insects. These observations were confirmed by analyzing the transcription profiles for the *N*-glycosylation-related genes (NGRGs). Expanding the analysis to the *N*-glycome of the adult BPH showed sex-specific *N*-glycosylation in insects. The data are discussed in relation to potential function(s) in development and sex specificity.

2. Materials and methods

2.1. Phylogenetic analysis

The NGRG protein sequences from *D. melanogaster* and *T. castaneum* were used as queries to search the unannotated *N. lugens* proteome (BioProject: PRJNA177647, Xue et al., 2014) using the BLAST tool from NCBI. Identified *Nilaparvata* orthologues were verified through InterProScan (Jones et al., 2014) and phylogenetic analysis were performed using RaxML v8.2.4 (Stamatakis, 2006) with known *Drosophila* and *Tribolium* protein sequences (Fig. S1). The protein sequences were aligned with MUSCLE using default settings in MEGA7 (Kumar et al., 2016). Maximum likelihood trees were build using the GTRGAMMA model with automated determination of the best amino acid substitution model, random number seed, and distinct starting tree. Bootstrap iterations were decided automatically. The corresponding genes were identified from the *N. lugens* genome database (BioProject: PRJNA177647, Xue et al., 2014) via tblastn using the BLAST tool from NCBI with the annotated *Nilaparvata* protein sequences. The amplified sequences of the corresponding genes were cloned (pJET1.2 cloning vector) and sequenced (LGC Genomics) to validate the predicted sequences.

2.2. Insect culture

A continuous colony of *N. lugens* was kept on 4- to 8-week-old rice plants (*Oryza sativa* japonica, Nipponbare, USDA Agricultural Research Service, Beltsville, MD) in a climate chamber under standard conditions of 27 ± 1 °C, 80 ± 5% relative humidity and a 16:8 light/dark photoperiod. Insects from 2nd instar (N2), 3rd instar (N3), 4th instar (N4) and 5th instar (N5) as well as adult insects (males and females) were collected and stored at −80 °C until further analysis.

2.3. Gene expression analysis

Approximately 15 mg of insects at different developmental stages (N3-N5) as well as adult males and females, were collected for RNA extraction. RNA was isolated using Qiagen RNeasy mini kit (Venlo, the Netherlands) according to the manufacturer's protocol. The TURBO DNA-free Kit (Ambion, Life technologies, Carlsbad, CA) was used to remove trace quantities of DNA. cDNA was synthesized with SuperScript III First-Strand Synthesis System (Invitrogen, Thermo Fisher Scientific, Carlsbad, CA) using 1 µg of total RNA. The cDNA was diluted 1:100 for subsequent real-time qPCR, which was performed using GoTaq qPCR Master Mix (Promega, Madison, WI) and CFX 96 Connect robot (BioRad, Hercules, CA). The program for thermal cycling included 10 s denaturation at 95 °C, 30 s annealing/extension at 58 °C with melting curve analysis at the end of the run. NlRps15 and NlTubulin were used as reference genes, based on in-house optimization. Detailed information on primer sequences and amplification efficiency can be found in Supplementary Table S1. The whole experiment was performed in three independent biological replications. Relative mRNA expression of the target genes was quantified by the BioRad CFX Manager software. Statistical analyses were performed by GraphPad Prism (La Jolla, CA). Primers for qPCR were designed using Primer blast tool (https://www.ncbi.nlm.nih.gov/tools/primer-blast/, Ye et al., 2012).

2.4. N-glycan purification

Protein extracts were made from approximately 100 mg of insect material. Whole insects were crushed in liquid nitrogen using a chilled mortar and pestle. Insect powder was dissolved in extraction buffer (4% SDS, 0.1 M DTT in 0.1 M Tris-HCl, pH 8.5) at a ratio of 10 ml/g of tissue. The samples were vortexed and sonicated for 3 min to lyse the insect cells. Subsequently, extracts were incubated for 3 min in boiling water and further sonicated for 5 min. After centrifugation at 16000 × *g* for 15 min, the supernatant was collected. Samples were prepared in at least three biological replicates. Tryptic peptides were prepared according to the filter-aided sample preparation method (Wiśniewski et al., 2009) with some small adjustments. In short, protein extracts were diluted with 8 M urea in 0.1 M Tris-HCl, pH 8.5 (urea buffer) and applied on an Amicon Ultra-0.5 centrifugal filter device (30 K; Millipore, Burlington, MA). After centrifugation for 15 min at 14000 × *g* the proteins on the filters were washed twice with urea buffer. Subsequently, 50 mM iodoacetamide was added and samples were incubated for 15 min at 37 °C in the dark. After alkylation, samples were washed 3 times with urea buffer, followed by three washes with 40 mM ammonium bicarbonate. Filter units were transferred into new collection tubes and trypsin (Pierce, Thermo Fisher Scientific, Waltham, MA) was added in a ratio of 1:100. Samples were incubated overnight at 37 °C. Resulting peptides were collected in 40 mM ammonium bicarbonate using centrifugation. Approximately 1.5–2 mg of tryptic peptides were treated with 0.3–0.4 mU peptide-*N*-glycosidase (PNGase) A from almonds (ProGlycAn, Vienna, Austria) in 50 mM citrate-phosphate buffer, pH 5. In contrast to PNGase F, PNGase A can also release core α1,3-fucosylated *N*-glycans from glycopeptides. Deglycosylation was performed at 37 °C for 20 h in a warm water bath. Released *N*-glycans were separated from the peptides on SepPak-C18 cartridges (Waters, Milford, MA) using the 1-propanol/5% acetic acid protocol (*N*-glycans in the flow-through) as described in Chalabi et al. (2006).

2.5. Mass spectrometry analysis

Samples were desalted using Glycoclean H-cartridges (Prozyme, Hayward, CA) according to manufacturer instructions and dried completely. Glycans were resuspended in labelling solution (750 mM $NaBH_3CN$, 175 mM 2-aminobenzamide (2-AB) in DMSO/acetic acid in a ratio of 10:3) and incubated for 2 h at 65 °C. Following 2-AB labeling, samples were purified using Glycoclean S-cartridges (Prozyme) according to manufacturer instructions and dried completely. Glycans were resuspended in 50% acetonitrile in water for MALDI-TOF analyses. MS analyses were performed on an Ultraflex II (Bruker, Bremen) mass spectrometer (6000 laser shots per spectrum) using the 2,5-DHB matrix (20 mg/ml in 50% acetonitrile, 0.1% trifluoroacetic acid). Equivolumes of matrix and sample (typically 1 µl) were mixed on plate

and allowed to dry. For each sample, three spots were analyzed and 3 mass spectra were recorded for each spot. The applied method has not been refined for charged glycans. Therefore conclusions can only be made about the presence of neutral *N*-glycans. Recorded spectra were analyzed using FlexAnalysis 3.4 (Bruker) and assigned peaks were annotated using GlycoWorkbench2 (Ceroni et al., 2008) based on *N*-glycans previously described in *D. melanogaster* and *T. castaneum*. *N*-glycan structures were grouped according to five main types: high mannose ($Man_{(5-9)}$, $Man_9Glc_{(1-3)}$), pauci-mannose ($Man_{(2-4)}$), monofucosylated ($Man_{(2-4)}Fuc_1$), difucosylated ($Man_{(2-4)}Fuc_2$) and complex (containing GlcNAc residues in the antennae) *N*-glycans. Differences between *N*-glycan groups in the various developmental stages were analyzed using SPSS Statistics 24 (ANOVA with Tukey's test or Kruskal-Wallis one-way ANOVA test).

2.6. Relative quantification of N-glycans in adult samples

About 0.5 pmol of the Glyko 2-AB NA3 (G3, Prozyme) standard was added to the nymphal and adult samples. New spectra were recorded on an Ultraflex II (Bruker) as described previously. At least 2 biological replicates were analyzed for the adult samples and three biological replicates were analyzed for N3 and N5. *N*-glycan intensity was normalized against the intensity of the added standard and corrected using the *N*-glycan (HexFuc) exhibiting the most stable signal in the different samples. Differences between adult male and female samples and nymphal samples were analyzed using SPSS Statistics 24 (Independent-Samples T-test or Mann-Whitney *U* test).

3. Results

3.1. High mannose and monofucosylated N-glycans are dominating the N-glycome of N. lugens

N-glycan profiles in *N. lugens* were determined for adults and different nymphal stages (N2 - N5). *N*-glycans were released from polypeptides by PNGase A and subsequently labeled with 2-AB. MALDI-TOF analysis yielded a total of 27 distinct glycan moieties (Table S2), which can be classified into five *N*-glycan groups: high mannose, pauci-mannose, monofucosylated, difucosylatedand complex *N*-glycans. Within both nymphal and adult *N*-glycomes high mannose and monofucosylated *N*-glycans represent the major glycan structures, accounting for approximately 70% of all *N*-glycans (Fig. 1). Pauci-mannose and complex *N*-glycans were less abundant and constituted around 15% and 10%, respectively, of the total *N*-glycan pool. Difucosylated *N*-glycans account for a minor fraction, with an appearance of around 1% of the total *N*-glycan profile. The complete list of identified *N*-glycans and their relative abundance is summarized for all studied life stages (Table S2).

3.2. The Nilaparvata N-glycome does not change during post-embryonal development, but reveals sex-specific N-glycosylation in adults

In holometabolous insects, the later stages of post-embryonal development are accompanied by changes in the protein *N*-glycosylation profile (Walski et al., 2016). To determine if such changes can also be observed during the post-embryonic development of hemimetabolous insects, the *N*-glycome of *N. lugens* was analyzed throughout the nymphal stages (N2-N5) (Fig. 1). Although small differences were observed in the relative abundance of pauci-mannose *N*-glycans between N2 and N4 (14.29 ± 0.79% and 19.65 ± 1.41%, respectively; $p = 0.034$) (Fig. S2), relative quantification, using an *N*-glycan standard, revealed no statistical differences ($p > 0.05$) for any of the detected *N*-glycans between N3 and N5 (Table S3).

Expanding this analysis to the adult *N*-glycan profile of female and male BPH revealed statistical differences in the relative abundance of all *N*-glycan groups between the two sexes (Fig. 1, Fig. S2). Except for

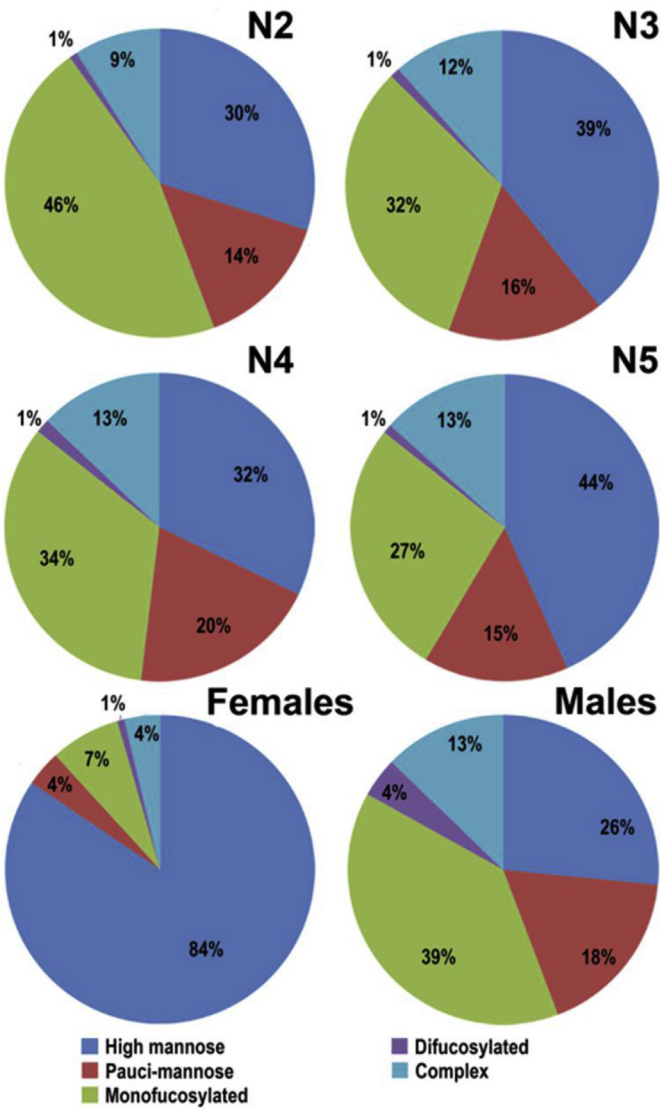

Fig. 1. *N*-glycan profiles of *N. lugens* throughout post-embryonic development and adult sexes. *N*-glycan profiles in *N. lugens* were determined for different nymphal stages (N2-N5) and adults (males and females) using MALDI-TOF analysis for at least three biological replicates. Pie charts show the relative abundance (%) of different *N*-glycan groups; high mannose, pauci-mannose, monofucosylated, difucosylated and complex *N*-glycans.

an increase in the relative abundance of difucosylated *N*-glycans, the profile of male adults resembled that of the nymphs (Fig. 1, Fig. S2). In contrast, the *N*-glycosylation in female adults progressed towards a unique *N*-glycan fingerprint (Fig. 1). To determine whether female planthoppers contain an increased level of high mannose glycans or rather show a decreased level of more processed glycans, the *N*-glycan profile of adult male and female adults was analyzed and quantified using an *N*-glycan standard (Table S4). These results showed a statistically relevant increase of about 10-fold for high mannose *N*-glycans (Hex_7-Hex_9) in females compared to males (Fig. 2A), with Hex_9 glycans being the dominant group (17-fold increase). In male adults, mono- and difucosylated pauci-mannose *N*-glycans were more prevalent compared to females (Fig. 2B). Complex $GalMan_3GlcNAc_3Fuc$ *N*-glycans were exclusively present in nymphs and adult males (Table S2), while the levels for difucosylated pauci-mannose *N*-glycans showed differences with the nymphal samples (Fig. S2). Relative quantification of the other *N*-glycans did not show any statistical differences between the two sexes (Table S4).

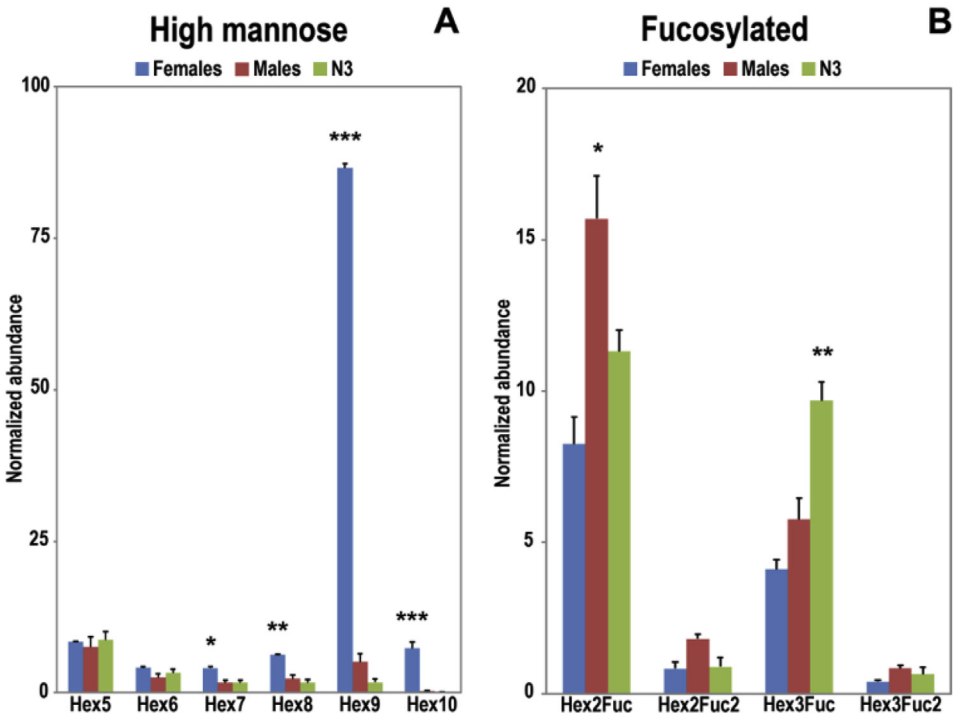

Fig. 2. True ratios of *N*-glycans in N3 and adult males and females of *N. lugens* compared to *N*-glycan standard. The *N*-glycans present in N3 and adults (males and females) were analyzed and quantified using an *N*-glycan standard. The normalized and corrected *N*-glycan abundance (mean ± SEM) for N3, male and female adults from at least two independent biological replicates is shown for high mannose *N*-glycans (A) and fucosylated pauci-mannose *N*-glycans (B). Statistical differences (Independent-Samples T-test or Mann-Whitney *U* test) are marked with an asterisk (*p < 0.05, ***p < 0.001).

3.3. Transcription levels of genes involved in protein N-glycosylation differ between sexes

Protein *N*-glycosylation is enabled via a complex and integrated sequence of enzymatic reactions. To check whether the transcription profile for the glycosyltransferases involved in the process of *N*-glycosylation can support the differences observed at *N*-glycan level, the putative NGRGs in the genome of *N. lugens* were identified through BLAST searches using the sequences from *D. melanogaster* and *T. castaneum* (Table 1). Transcription levels were quantified in both nymphal and adult stages of BPH (Fig. S3). During nymphal development, the transcription levels of most NGRGs were constant (Fig. S3), confirming the stable *N*-glycan profile observed throughout the different nymphal stages. The only exception was β4GalNAc transferase A (β4GalNAcTA) for which the transcription levels decreased during nymphal development. However, the *N*-glycans generated by the enzyme activity of the β4GalNAcTA gene ($Hex_4HexNAc_2Fuc$ and $Hex_3HexNAc_3Fuc$) were very low abundant and did not differ significantly between the N3 and N5 stages (Table S3). Throughout all life stages, nymphs and adults, the genes encoding enzymes involved in *N*-glycan attachment to the protein (Ostt3a/b) showed similar transcription levels (Fig. S3), suggesting an important role of *N*-glycosylation in the proper functioning of the cell. In adult males, an increased expression of genes involved in initial trimming (GCS1, Man1a) and further modification (Man2a/2b, Mgat 1/2/4, FucT6/A, β4GalNAcTB and ST6Gal) was present compared to adult females (Fig. S3). The lower transcription levels for genes coding for enzymes involved in initial trimming in females might account for the presence of glucosylated *N*-glycans (Hex_{10-12}) in these samples (Table S2). No statistical differences were observed in the transcription levels of GCS2, Man1b, Fdl and β4GalNAcTA. Comparative analysis of the transcription profiles for all NGRGs revealed a clear clustering for the male and female samples in two separate branches (Fig. 3).

4. Discussion

In holometabolous insects, *N*-glycosylation of proteins plays an important role in different biological processes such as development, immunity and fertility (Walski et al., 2017). Previous studies in *D. melanogaster* and *T. castaneum* have shown that the transition from immature larvae to adults is accompanied with a change in protein *N*-glycosylation (Sarkar et al., 2006; Arakane et al., 2011; Walski et al., 2016). Adult beetles and flies contain more processed *N*-glycans than larvae, while the levels of difucosylated and complex *N*-glycans do not differ much (Fabini et al., 2001; Aoki et al., 2007; Walski et al., 2016). In agreement, most genes coding for the enzymes involved in the *N*-glycosylation process show increased transcription levels during later developmental stages with the highest expression levels appearing particularly during the pupal stage (Walski et al., 2016). Furthermore, silencing of these NGRGs resulted in developmental phenotypes such as larval mortality, and prevention of pupation and adult eclosion. Variations in the total *N*-glycan profile have also been observed for different developmental stages of the nematode *Caenorhabditis elegans*, suggesting that changes in glycosylation profiles during post-embryonic development may be widespread among invertebrates (Cipollo et al., 2005). In this study, the *N*-glycan profile for different post-embryonic life stages of a hemimetabolous insect was studied in *N. lugens*, a notorious pest insect of rice. In contrast to the changes in the *N*-glycan profile observed during the post-embryonic development in holometabolous insects, the *N*-glycome of *N. lugens* did not change during nymphal development. Interestingly, these data are in agreement with the transcription profiles for NGRGs, showing stable transcription levels for most genes throughout development. Although no changes in *N*-glycosylation were observed during post-embryonal development, protein *N*-glycosylation might still be essential for the development of hemimetabolous insects, and silencing may lead to lethal and sublethal effects such as developmental arrest or growth defects. Further research is therefore needed to elucidate the importance of protein *N*-glycosylation during post-embryonic development of hemimetabolous insects, and its use as novel insecticidal target to control important pest insects.

Expanding the study of the non-reproductive nymphal stages with the analysis of the *N*-glycan profiles for male and female adults of *N. lugens*, revealed sex-specific *N*-glycosylation in insects. In humans, sex and age specificity of protein *N*-glycosylation has already been described for *N*-glycomes from plasma (Knezević et al., 2009) and saliva (Qin et al., 2013). Sex-related variations in the *N*-glycome have recently been reported for the porcine nodule worm *Oesophagostomum dentatum*

Table 1
Overview of putative *N*-glycosylation-related genes in *N. lugens*. or GlcNAc – *N*-acetylglucosamine, or Man – mannose, or Glc – glucose, or Fuc – fucose, or GalNAc – *N*-acetylgalactosamine, or Gal – galactose, or Sia – sialic acid, Asn – asparagine in a polypeptide chain. Table adjusted from Walski et al. (2016).

Protein name	Gene name	*Drosophila* accession	*Tribolium* Accession	*Nilaparvata* accession	Function
Oligosaccharyltransferase (OST) complex	Ostt3a Ostt3b	Q9VRE0 Q9XZ53	TC010433 TC009183	NLU006107.1 NLU011128.1	Attachment of *N*-glycan precursor from dolichol to a polypeptide
α-Glucosidase I α-Glucosidase II	GCS1 GCS2	Q9VZ04Q7KMM4	TC011354 TC032148	NLU018489.1 NLU010177.1	Trimming of terminal glucose residues from *N*-glycan
Golgi α-1,2-mannosidase Ia Golgi α-1,2-mannosidase Ib	Man1a Man1b	P53624 Q9VAP8	TC011089 TC002991	NLU026219.1 NLU014338.1	Initial trimming of terminal mannose residues from Man9 to Man5
Mannosyl(α-1,3)-glycoprotein β-1,2-N-acetylglucosaminyl-transferase I	Mgat1	Q60GL7	TC009001	NLU007274.1	GlcNAc transferase
Golgi α-mannosidase IIa Golgi α-mannosidase IIb	Man2a Man2b	A0A0B4KFG0 Q9VF33	TC009186 TC014283	NLU004974.2 NLU023574.1	Trimming of mannose residues for the production of pauci-mannose *N*-glycans
N-acetylhexosaminidase	Fdl	Q8WSF3	TC009779	NLU008747.1	Removing of terminal GlcNAc
Core α1,6-fucosyltransferase Core α1,3-fucosyltransferase	FucT6 FucTA	Q9VYV5 Q9VUL9	TC008521 TC014343	NLU008004.2 NLU006240.1	Adding fucose at core structure of *N*-glycan with formation of either mono- or difucosylated *N*-glycans
Mannosyl(α-1,3)-glycoprotein β-1,2-N-acetylglucosaminyl-transferase II Mannosyl(α-1,3)-glycoprotein β-1,2-N-acetylglucosaminyl-transferase IV	Mgat2 Mgat4	Q961U0 Q9VUH4	TC001867 TC003870	NLU006734.1 NLU008250.1	GlcNAc transferases involved in production of complex *N*-glycans
β4GalNAc transferase A β4GalNAc transferase B	β4GalNAcTA β4GalNAcTB	Q7KN92 Q9VAQ8	TC006388 TC006987	NLU022128.1 NLU029089.1	Addition of Gal or GalNAc for the production of complex *N*-glycans
Sialyltransferase	ST6Gal	Q9W121	TC014265	NLU028253.1	Sialic acid transferase

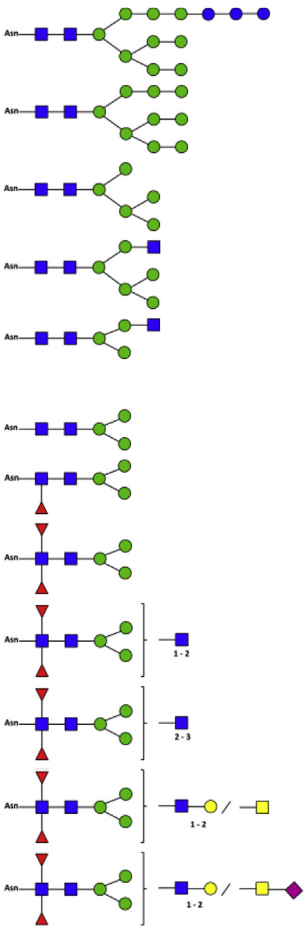

(Jiménez-Castells et al., 2016), but sex specificity of protein *N*-glycosylation has not yet been described in insects. In *N. lugens*, male adults retain a glycan profile similar to that of the nymphal stages, except for a slight increase in difucosylated pauci-mannose *N*-glycans. In the fruit fly, these difucosylated *N*-glycans are mainly present in neural tissues and male reproductive organs (Rendić et al., 2006). Based hereon, the small increase of difucosylated *N*-glycans in adult males can suggest a role for glycoproteins carrying difucosylated glycans in the *Nilaparvata* male reproductive system. In contrast, the *N*-glycome of adult females progresses from the nymphal profile towards a female-unique *N*-glycosylation pattern. Compared to males, female *N*-glycomes contain a striking increase in high mannose *N*-glycans and a decrease in mono- and difucosylated pauci-mannose *N*-glycans. In agreement to this, increased transcription levels for NGRGs involved in the initial trimming and further processing of the *N*-glycans were observed in male adults, resulting in the formation of less unprocessed *N*-glycan forms. Glycoproteins carrying high mannose *N*-glycans may play a role in the female reproductive system. For example, vitellogenin and vitellogenin receptor, two proteins involved in the female reproductive process, are known to be decorated with high mannose *N*-glycans (Sappington et al., 1996; Ciudad et al., 2005; Tufail and Takeda, 2008; Zhang et al., 2016). While transcription profiles of NGRGs for different nymphal stages as well as between male and female adults show consistency with the obtained *N*-glycan profiles, a discrepancy is observed between the *N*-glycan profile and the transcript profile when comparing nymphal and adult stages. Although male adults and nymphal stages yield a similar *N*-glycan profile, the transcription profiles for the NGRGs in nymphs are more similar to that of the female adults.

In conclusion, we evaluated the *N*-glycome of a hemimetabolous pest insect throughout development and between the two sexes. In contrast to holometabolous insects where changes in the *N*-glycosylation pattern during the later stages of post-embryonic development are crucial for the transition to adult, the *N*-glycome does not change during the post-embryonic life stages of *N. lugens*. Intriguingly, the influence of the sexes on *N*-glycosylation was demonstrated by the apparent shift in the *N*-glycan profile from male to female adults, showing sex-related *N*-glycosylation in insects. While male adults retained an *N*-glycan profile resembling the nymphal pattern, females obtained a unique *N*-glycan fingerprint characterized by a striking increase in high mannose *N*-glycans. This research lays a foundation to further explore the differences in post-embryonic development between holo- and hemimetabolous insects and can contribute to the discovery of new, exciting physiological pathways diverging between male and female adults.

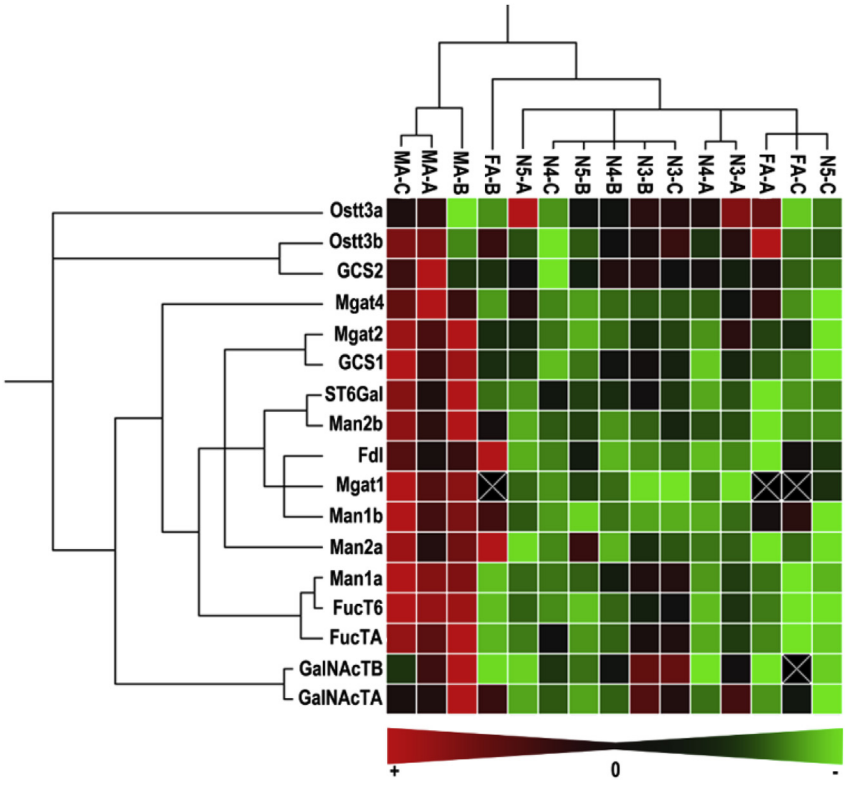

Fig. 3. Clustergram of NGRGs of *N. lugens*. Expression of NGRGs during development (N3-N5) and through adult sexes; male adult (MA), female adult (FA). Relative gene expression was quantified using qRT-PCR with NlRps15 and NlTubulin as reference genes. The data are shown in a hierarchy based on the degree of similarity of expression for different samples and targets; upregulation (red), downregulation (green), no regulation (black) or no value (black with a white X). Data are derived from three biological replicates (a–c). (For interpretation of the references to colour in this figure legend, the reader is referred to the Web version of this article.)

Notes

The authors declare no competing financial interests.

Author contributions

FS performed the *N*-glycome analysis and analyzed the data. NS and EDP provided the mass spectrometry facility and helped with the MS analysis. FS, KDS, NY and YS identified the NGRGs and performed the phylogenetic analysis. FS and YS analyzed the transcription profiles. EVD and GS supervised the study and were involved in critical analysis of the data, manuscript corrections and discussion. All co-authors contributed to the writing and correction of the manuscript. All authors read and approved the final manuscript.

Funding

This research was funded by the Research Foundation Flanders (Belgium), the Special Research Fund from the Ghent University (Belgium), the FNRS (Belgium) and the Walloon region (Belgium). The authors would like to acknowledge Miss Dominique Baiwir (GIGA Proteomics facility, U.Liège) for helpful discussions about relative quantification.

Appendix A. Supplementary data

Supplementary data to this article can be found online at https://doi.org/10.1016/j.ibmb.2019.01.008.

Abbreviations

Asn	Asparagine
BPH	brown planthopper
ER	endoplasmic reticulum
N5	fifth instar
N4	fourth instar
Fuc	fucose
FucT	fucosyl transferase
Fdl	fused lobes
Gal	galactose
Glc	glucose
GCS	glucosidase
Man	mannose
Man	mannosidase
GalNAc	*N*-acetyl galactosamine
GlcNAc	*N*-acetyl glucosamine
Mgat	*N*-acetyl glucosaminyl transferase
NGRG	*N*-glycosylation-related genes
Ostt	oligosaccharyl transferase
PNGase A	peptide-*N*-glycosidase A
PNGase F	peptide-*N*-glycosidase F
N2	second instar
Sia	sialic acid
ST6Gal	sialyl transferase
N3	third instar

References

Altmann, F., 1996. N-glycosylation in insects revisited. Trends Glycosci. Glycotechnol. 8, 101–114.

Aoki, K., Perlman, M., Lim, J.M., Cantu, R., Wells, L., Tiemeyer, M., 2007. Dynamic developmental elaboration of N-linked glycan complexity in the *Drosophila melanogaster* embryo. J. Biol. Chem. 282, 9127–9142.

Arakane, Y., Baguinon, M.C., Jasrapuria, S., Chaudhari, S., Doyungan, A., Kramer, K.J., Muthukrishnan, S., Beeman, R.W., 2011. Both UDP N-acetylglucosamine pyrophosphorylases of *Tribolium castaneum* are critical for molting, survival and fecundity. Insect Biochem. Mol. Biol. 41, 42–50.

Bao, Y.Y., Qu, L.Y., Zhao, D., Chen, L.B., Jin, H.Y., Xu, L.M., Cheng, J.A., Zhang, C.X., 2013. The genome- and transcriptome-wide analysis of innate immunity in the brown planthopper, *Nilaparvata lugens*. BMC Genomics 14. https://doi.org/10.1186/1471-2164-14-160.

Ceroni, A., Mass, K., Geyer, H., Geyer, R., Dell, A., Haslam, S.M., 2008. GlycoWorkbench: a tool for the computer-assisted annotation of mass spectra of glycans. J. Proteome Res. 7, 1650–1659.

Chalabi, S., Panico, M., Sutton-Smith, M., Haslam, S.M., Patankar, M.S., Lattanzio, F.A., Morris, H.R., Clark, G.F., Dell, A., 2006. Differential O-glycosylation of a conserved

domain expressed in murine and human ZP3. Biochemistry 45, 637–647.
Cipollo, J.F., Awad, A.M., Costello, C.E., Hirschberg, C.B., 2005. N-glycans of *Caenorhabditis elegans* are specific to developmental stages. J. Biol. Chem. 280, 26063–26072.
Ciudad, L., Piulachs, M.D., Bellés, X., 2005. Systemic RNAi of the cockroach vitellogenin receptor results in a phenotype similar to that of the *Drosophila* yolkless mutant. FEBS J. 273, 325–335.
De Pourcq, K., De Schutter, K., Callewaert, N., 2010. Engineering of glycosylation in yeast and other fungi: current state and perspectives. Appl. Microbiol. Biotechnol. 87, 1617–1631.
Dönitz, J., Schmitt-Engel, C., Grossmann, D., Gerischer, L., Tech, M., Schoppmeier, M., Klingler, M., Bucher, G., 2014. iBeetle-base: a database for RNAi phenotypes in the red flour beetle *Tribolium castaneum*. Nucleic Acids Res. 43, D720–D725.
Dwek, A., 1996. Glycobiology: toward understanding the function of sugars. Chem. Rev. 96, 683–720.
Endo, T., 2009. New era of glycoscience: intrinsic and extrinsic functions performed by glycans. Biol. Pharm. Bull. 32, 767–773.
Fabini, G., Freilinger, A., Altmann, F., Wilson, I.B., 2001. Identification of core α1,3-fucosylated glycans and cloning of the requisite fucosyltransferase cDNA from *Drosophila melanogaster*. J. Biol. Chem. 276, 28058–28067.
Jiménez-Castells, C., Vanbeselaere, J., Kohlhuber, S., Ruttkowski, B., Joachim, A., Paschinger, K., 2016. Gender and developmental specific N-glycomes of the porcine parasite *Oesophagostomum dentatum*. Biochim. Biophys. Acta 1861, 418–430.
Jones, P., Binns, D., Chang, H.Y., Fraser, M., Li, W., McAnulla, C., McWilliam, H., Maslen, J., Mitchell, A., Nuka, G., Pesseat, S., Quinn, A.F., Sangrador-Vegas, A., Scheremetjew, M., Yong, S.Y., Lopez, R., Hunter, S., 2014. InterProScan 5: genome-scale protein function classification. Bioinformatics 30, 1236–1240.
Kajihura, H., Hamaguchi, Y., Mizushima, H., Misaki, R., Fujiyama, K., 2015. Sialylation potentials of the silkworm, *Bombyx mori; B. mori* possesses an active α2,6-sialyl-transferase. Glycobiology 25, 1441–1453.
Knezević, A., Polasek, O., Gornik, O., Rudan, I., Campbell, H., Hayward, C., Wright, A., Kolcic, I., O'Donoghue, N., Bones, J., Rudd, P.M., Lauc, G., 2009. Variability, heritability and environmental determinants of human plasma N-glycome. J. Proteome Res. 8, 694–701.
Kshirod, K.J., Suk-Man, K., 2010. Current status of brown planthopper (BPH) resistance and genetics. Rice 3, 161–171.
Kubelka, V., Altmann, F., Staudacher, E., Tretter, V., März, L., Hård, K., Kamerling, J.P., Vliegenthart, J.F., 1993. Primary structures of the N-linked carbohydrate chains from honeybee venom phospholipase A2. Eur. J. Biochem. 213, 1193–1204.
Kubelka, V., Altmann, F., März, L., 1995. The asparagine-linked carbohydrate of honeybee venom hyaluronidase. Glycoconj. J. 12, 77–83.
Kumar, S., Stecher, G., Tamura, K., 2016. MEGA7: molecular evolutionary genetics analysis version 7.0 for bigger datasets. Mol. Biol. Evol. 33, 1870–1874.
Kurz, S., Aoki, K., Jin, C., Karlsson, N.G., Tiemeyer, M., Wilson, I.B., Paschinger, K., 2015. Targeted release and fractionation reveal glucoronylated and sulphated N- and O-glycans in larvae of dipteran insects. J. Proteomics. 126, 172–188.
Li, J., Chen, Q., Lin, Y., Jiang, T., Wu, G., Hua, H., 2011. RNA interference in *Nilaparvata lugens* (Homoptera: Delphacidae) based on dsRNA ingestion. Pest Manag. Sci. 67, 852–859.
Mabashi-Asazuma, H., Sohn, B.H., Kim, Y.S., Kuo, C.W., Khoo, K.H., Kucharski, C.A., Fraser Jr., M.J., Jarvis, D.L., 2015. Targeted glycoengineering extends the protein N-glycosylation pathway in the silkworm silk gland. Insect Biochem. Mol. Biol. 65, 20–27.
North, S.J., Koles, K., Hembd, C., Morris, H.R., Dell, A., Panin, V.M., Haslam, S.M., 2006. Glycomic studies of *Drosophila melanogaster* embryos. Glycoconj. J. 23, 345–354.
Ohtsubo, K., Marth, J.D., 2006. Glycosylation in cellular mechanisms of health and disease. Cell 126, 855–867.
Qin, Y., Zhong, Y., Zhu, M., Dang, L., Yu, H., Chen, Z., Chen, W., Wang, X., Zhang, H., li, Z., 2013. Age- and sex-associated differences in the glycopatterns of human salivary glycoproteins and their roles against influenza A virus. J. Proteome Res. 12, 2742–2754.
Rendić, D., Linder, A., Paschinger, K., Borth, N., Wilson, I.B., Fabini, G., 2006. Modulation of neural carbohydrate epitope expression in *Drosophila melanogaster* cells. J. Biol. Chem. 281, 3343–3353.
Sanderson, M.J., 2008. Phylogenetic signal in the eukaryotic tree of life. Science 321, 121–123.
Sappington, T.W., Kokoza, V.A., Cho, W.L., Raikhel, A.S., 1996. Molecular characterization of the mosquito vitellogenin receptor reveals unexpected high homology to the *Drosophila* yolk protein receptor. Proc. Natl. Acad. Sci. U.S.A. 93, 8934–8939.
Sarkar, M., Leventis, P.A., Silvescu, C.I., Reinhold, V.N., Schachter, H., Boulianne, G.L., 2006. Null mutations in *Drosophila* N-acetylglucosaminyltransferase I produce defects in locomotion and a reduced life span. J. Biol. Chem. 281, 12776–12785.
Schiller, B., Hykollari, A., Yan, S., Paschinger, K., Wilson, I.B., 2012. Complicated N-linked glycans in simple organisms. J. Biol. Chem. 393, 661–673.
Soya, S., Sahar, U., Karaçali, S., 2016. Monosaccharide profiling of silkworm (*Bombyx mori* L.) nervous system during development and aging. Invertebr. Neurosci. 16. https://doi.org/10.1007/s10158-016-0191-6.
Stamatakis, A., 2006. RAxML-VI-HPC: maximum likelihood-based phylogenetic analyses with thousands of taxa and mixed models. Bioinformatics 22, 2688–2690.
Stanton, R., Hykollari, A., Eckmair, B., Malzl, D., Dragosits, M., Palmberger, D., Wang, P., Wilson, I.B., Paschinger, K., 2017. The underestimated N-glycomes of lepidopteran species. Biochim. Biophys. Acta 1861, 699–714.
Ten Hagen, K.G., Zhang, L., Tian, E., Zhang, Y., 2009. Glycobiology on the fly: developmental and mechanistic insights from *Drosophila*. Glycobiology 19, 102–111.
Tufail, M., Takeda, M., 2008. Molecular characteristics of insect vitellogenins. J. Insect Physiol. 54, 1447–1458.
Varki, A., Kornfield, S., 2017. Historical background and overview. In: Varki, A. (Ed.), Essentials in Glycobiology. Cold Spring Harbor., New York, pp. 1–18.
Walski, T., Van Damme, E.J.M., Smargiasso, N., Christiaens, O., De Pauw, E., Smagghe, G., 2016. Protein N-glycosylation and N-glycan trimming are required for post-embryonic development of the pest beetle *Tribolium castaneum*. Sci. Rep. 6. https://doi.org/10.1038/srep35151.
Walski, T., De Schutter, K., Van Damme, E.J.M., Smagghe, G., 2017. Diversity and functions of protein glycosylation in insects. Insect Biochem. Mol. Biol. 83, 21–34.
Wilson, I.B., 2002. Glycosylation of proteins in plants and invertebrates. Curr. Opin. Struct. Biol. 12, 569–577.
Wiśniewski, J.R., Zougman, A., Nagarajuna, N., Mann, M., 2009. Universal sample preparation method for proteome analysis. Nat. Methods 6, 359–363.
Xue, J., Zhou, X., Zhang, C.X., Yu, L.L., Fan, H.W., Wang, Z., Xu, H.J., Xi, Y., Zhu, Z.R., Zhou, W.W., Pan, P.L., Li, B.L., Colbourne, J.K., Noda, H., Suetsugu, Y., Kobayashi, T., Zheng, Y., Liu, S., Zhang, R., Liu, Y., Luo, Y.D., Fang, D.M., Chen, Y., Zhan, D.L., Lv, X.D., Cai, Y., Wang, Z.B., Huang, H.J., Cheng, R.L., Zhang, X.C., Lou, Y.H., Yu, B., Zhuo, J.C., Ye, Y.X., Zhang, W.Q., Shen, Z.C., Yang, H.M., Wang, J., Wang, J., Bao, Y.Y., Cheng, J.A., 2014. Genomes of the rice pest brown planthopper and its endosymbionts reveal complex complementary contributions for host adaptation. Genome Biol. 15. https://doi.org/10.1186/s13059-014-0521-0.
Ye, J., Coulouris, G., Zaretskaya, I., Cutcutache, I., Rozen, S., Madden, T.L., 2012. Primer-blast: a tool to design target-specific primers for polymerase chain reaction. BMC Bioinf. 13. https://doi.org/10.1186/1471-2105-13-134.
Zhang, W., Ma, L., Xiao, H., Xie, B., Smagghe, G., Guo, Y., Liang, G., 2016. Molecular characterization and function analysis of the vitellogenin receptor from the cotton bollworm, *Helicoverpa armigera* (Hübner) (Lepidoptera, Noctuidae). PLoS One 11. https://doi.org/10.1371/journal.pone.0155785.